Trop J Nat Prod Res, May 2025; 9(5): 1964 - 1972 **ISSN 2616-0684 (Print)**
ISSN 2616-0692 (Electronic)

Tropical Journal of Natural Product Research

Available online at https://www.tjnpr.org

Original Research Article

Exploring the *In Vitro* Anti-Inflammatory Effect and *In Silico* Toxicity Profile of *Curcuma aeruginosa* Roxb. Extract in RAW 264.7 Macrophages

Defiona RNAzerlyn[1], Dinia R Dwijayanti[1,2], Masruri Masruri[3], Nashi Widodo[1]*

[1]*Department of Biology, Faculty of Mathematics and Natural Sciences, Universitas Brawijaya, Malang, 65145, Indonesia*
[2]*Research Center of Complementary Medicine and Functional Food, Universitas Brawijaya, Malang, 65145, Indonesia*
[3]*Department of Chemistry, Faculty of Mathematics and Natural Sciences, Universitas Brawijaya, Malang, 65145, Indonesia*

ARTICLE INFO

Article history:
Received 17 November 2024
Revised 23 January 2025
Accepted 21 April 2025
Published online 01 June 2025

ABSTRACT

Chronic inflammation is implicated in numerous diseases, and targeting pro-inflammatory pathways is a promising therapeutic approach. *Curcuma aeruginosa* Roxb. known for its traditional medicinal uses, contains sesquiterpenes that may offer anti-inflammatory benefits. This study examines the anti-inflammatory properties of ethanol extract from *C. aeruginosa* Roxb. rhizome on nitric oxide (NO) production in LPS-stimulated RAW 264.7 macrophages using *in vitro* and *in silico* approaches. The *in vitro* analysis was conducted by treating RAW 264.7 cells with varying concentrations of the extract (15, 30, and 60 µg/mL), followed by NO measurement using the Griess assay to evaluate inhibition. The IC_{50} value of the extract was determined to be 29.03 ± 4.37 µg/mL. Notably, cell viability analysis using the WST-1 assay confirmed that these treatment concentrations did not induce toxicity in the cells. In the *in silico* analysis, 17 sesquiterpene compounds identified from the extract were screened for bioactivity and toxicity, then tested in molecular docking and molecular dynamics simulations with primary inflammatory proteins, including iNOS, IKK*β*, ERK2, JNK1, and p38. Molecular docking and molecular dynamics results highlighted three key compounds, which were dehydrochromolaenin, pyrocurzerenone, and turmeronol B at exhibited strong binding affinities, particularly with iNOS, indicating stable interactions with significant anti-inflammatory potential. These findings suggest that *C. aeruginosa* rhizome extract effectively reduces NO production *in vitro* and demonstrates molecular interactions that inhibit inflammatory mediators *in silico*. This extract holds potential as a natural anti-inflammatory agent with a multifaceted mechanism of action against inflammatory signaling pathways.

Keywords: Antiinflammatory, *Curcuma aeruginosa* Roxb., Lipopolysaccharide, Nitric oxide, RAW 264.7

Introduction

Inflammation is the body's primary defense mechanism to tissue injury caused by infections, cell damage, and stimulation by various allergens and irritants. The primary objective of the inflammatory process is to eliminate pathogens and initiate the healing process.[1] Chronic inflammation arises when the body fails to control tissue damage during acute inflammation, leading to widespread tissue damage across various body systems. This chronic inflammatory state can result in numerous diseases, such as sepsis, asthma, obesity, type 2 diabetes, neurodegenerative diseases like Alzheimer's, cancer, Crohn's disease, polyarthritis rheumatoid, cardiovascular diseases like atherosclerosis and cardiac ischemia, and autoimmune diseases.[2]
Inflammation can occur through distinct signaling pathways within each cell type and location in the body. Lipopolysaccharide (LPS), a component of the outer cell wall of Gram-negative bacteria, is a well-known stimulant of inflammation. It activates TLR4 and initiates inflammatory signaling pathways like mitogen-activated protein kinase (MAPK) and nuclear factor-κB (NF-κB). These pathways then lead to the production of inflammatory cytokines, including interleukin-1*β* (IL-1*β*), interleukin-6 (IL-6), tumor necrosis factor-*α* (TNF-*α*), and other pro-inflammatory molecules such as prostaglandin-E2 (PGE2) and nitric oxide (NO) which are implicated in tissue damage and pathological processes.[1,4]
Various therapeutic strategies address inflammation, one of which involves the use of Non-Steroidal Anti-Inflammatory Drugs (NSAIDs). These drugs act by non-selectively inhibiting the activity of cyclooxygenase enzymes (COX-1 and COX-2), reducing prostaglandin (PG) production. However, excessive and long-term NSAID use can lead to adverse effects on tissues or cells[2,5] One significant side effect of NSAIDs is upper gastrointestinal damage, manifesting symptoms such as abdominal pain, gastroduodenal ulcers, varying levels of dyspepsia, bleeding or perforation, nonspecific colitis, and other conditions. Additionally, NSAIDs may lead to hepatic reactions, hepatotoxicity, liver damage, cardiovascular disorders, peripheral edema, and hyperkalemia.[6] In response, alternative therapies with antiinflammatory benefits and reduced toxicity are increasingly in demand.
Herbal plants form a vital foundation of traditional medicine worldwide, with much of the global population relying on herbal plants as alternative treatments for various diseases due to their accessibility, affordability, and minimal side effects. Herbal plant-based alternatives for chronic inflammatory diseases are essential to minimize side effects and enhance efficacy through the optimal minimum dosage.[7, 8] One commonly used plant is *Curcuma aeruginosa* Roxb. This plant native to Southeast Asia and widely distributed in countries such as Indonesia,

***Corresponding author. E mail: widodo@ub.ac.id
Tel.: +62 813 2597 0829

Citation: Azerlyn DRN, Dwijayanti DR, Masruri M, Widodo N. Exploring the In Vitro Anti-Inflammatory Effect and In Silico Toxicity Profile of *Curcuma aeruginosa* Roxb. Extract in RAW 264.7 Macrophages. Trop J Nat Prod Res. 2025; 9(5): 1964 – 1972. https://doi.org/10.26538/tjnpr/v9i5.12

Official Journal of Natural Product Research Group, Faculty of Pharmacy, University of Benin, Benin City, Nigeria

Japan, Malaysia, Thailand, China, and South India. *C. aeruginosa* Roxb., known as temu ireng in Indonesia, has an aromatic rhizome with a distinctive ginger-like aroma. It is widely used in ethno-medicine to address various ailments, including digestive disorders, wounds, rheumatism, dysmenorrhea, fever, cough, and asthma. The rhizome of *C. aeruginosa* Roxb. contains 34 chemical compounds, including 5 flavonoids, 26 terpenoids, and 3 diarylheptanoids, as well as essential oils with 232 volatile compounds found in both the leaves and rhizomes. Additionally, *C. aeruginosa* Roxb. exhibits multiple bioactivities, including anticancer, antimicrobial, antioxidant, anti-dengue, immunostimulant, and anti-inflammatory properties.[7,9]

Previous studies have explored the inhibition of NO production by *C. aeruginosa* Roxb. extract in LPS-stimulated RAW 264.7 macrophage cells, demonstrating its anti-inflammatory potential. However, the existing studies primarily focus on general observations of NO reduction without addressing the specific molecular interactions or signaling pathways influenced by the bioactive compounds of *C. aeruginosa* Roxb. Moreover, the interaction of these compounds with key proteins within the MAPK and NF-κB signaling pathways, which regulate inflammatory responses, remains inadequately understood. This knowledge gap presents a unique opportunity to uncover novel mechanisms underlying the anti-inflammatory properties of *C. aeruginosa* Roxb. Consequently, this study investigates the effect of *C. aeruginosa* Roxb. rhizome extract on NO production in LPS-stimulated RAW 264.7 cells while also utilizing computational approaches to identify specific bioactive compounds and their potential molecular targets. By integrating experimental and *in silico* methodologies, this research aims to elucidate the anti-inflammatory mechanisms of *C. aeruginosa* Roxb., thereby contributing to its development as a safer and more effective alternative therapy for inflammation-related diseases.

Materials and Methods

Extraction of C. aeruginosa Roxb. Rhizome

The dried powder of *C. aeruginosa* Roxb. rhizome was obtained from UPT Material Medika Batu, East Java, Indonesia (7°52'03"S 112°31'09"E). The extraction process was conducted using maceration, following previous study.[10] The powdered simplicia was extracted with 95% ethanol overnight and in dark conditions. This extraction was repeated three times. After extraction, the solution was filtered through Whatman No. 1 filter paper (Whatman Ltd., England). The *C. aeruginosa* Roxb. ethanol extract (hereinafter: CRE) was then evaporated using a rotary evaporator (Buchi R-210 Rotavapor System, Thermo Scientific, US) at 40°C until a crude extract in paste form was obtained. The resulting extract in paste form was stored in an airtight bottle in a freezer at 4°C for further analysis.

RAW 264.7 Cell Line Culture

RAW 264.7 cell lines were cultured in a 60 mm culture dish using DMEM-HG (Dulbecco's Modified Eagle Medium-High Glucose) (Sigma-Aldrich, Co., Merck KgaA) enriched with 10% FBS (Fetal Bovine Serum) (Sigma-Aldrich, Co., Merck KgaA) and 1% Penstrep (Penicillin-Streptomycin) antibiotics (Sigma-Aldrich, Co., Merck KgaA). The cell culture was incubated in a 5% CO_2 incubator at 37°C in a humidified condition. The culture was maintained every two days until it reached a stable and confluent state.

Griess Assay

Nitrite levels were determined using the Griess assay, following the method as described in a previous study[11]. RAW 264.7 cells were seeded at a density of 1×10^5 cells/mL in a 24-well plate and incubated at 37°C with 5% CO_2 for 24 hours. Post-incubation, the cells were treated with 15, 30, and 60 µg/mL of CRE and inflammation was stimulated by treating cells with 1 µg/mL LPS (Sigma-Aldrich, Co., Merck KGaA). Subsequently, 75 µL of the culture supernatant from the treated cells was collected and transferred to a 96-well plate and was mixed with 75 µL freshly prepared Griess reagent modified (Sigma-Aldrich, USA; G4410) contained (0.5% sulfanilamide and 0.005% naphthylethylenediamine dihydrochloride in 2.5% phosphoric acid). $NaNO_2$ (sodium nitrite) solutions with concentrations of 0, 25, 50, 75, and 100 µg/mL were used as standard solutions. The absorbance values were read at a wavelength of 540 nm using a microplate reader (Multiskan SkyHigh Microplate Spectrophotometer, Thermo Scientific, US). Nitrite levels in the samples were interpolated from a standard curve.

Cell Viability Assay

The cell viability assay was conducted using the Water-Soluble Tetrazolium Salt (WST-1) method following previous study[11]. The remaining media in the well plate after nitrite measurement was discarded. The cells in the wells were then treated with WST-1 reagent (Sigma-Aldrich, USA) at a 5% concentration. The cells were incubated in the dark for 30 minutes. Subsequently, 100 µL of the supernatant was transferred to a 96-well plate. A complete DMEM medium was used as the blank solution. The absorbance values were read at a wavelength of 450 nm using a microplate reader (Multiskan SkyHigh Microplate Spectrophotometer, Thermo Scientific, US). The percentage of viable cells after treatment was determined by comparing it to the control group.

Statistical Analysis

Data analysis for NO assay results were represented from three independent experiments. Each experiment was done by using different cell line passages. Each experiment included technical triplicates for every condition. Experimental differences were assessed using Student's t-test ($P < 0.05$ and $P < 0.01$) and were expressed as means ± standard deviation (SD).

Prediction of Bioactivity and Toxicity of Compounds

Data of compounds from CRE were obtained from previous literature. The compounds were selected based on bioactivity and toxicity potential related to inflammation. Bioactivity screening of compounds was conducted through the web server PASS Online Way2drug (https://www.way2drug.com/passonline/).[12] The Probability active (Pa) value of each compound was selected based on activities such as anti-inflammatory, immunosuppressant, nitric oxide scavenger, JAK2 expression inhibitor, transcription factor NF kappa B inhibitor, MMP9 expression inhibitor, nitrite reductase (NO-forming) inhibitor, antioxidant, free radical scavenger, prostaglandin-E2 9-reductase, nitric oxide antagonist, NOS2 expression inhibitor, and TNF expression inhibitor. Compounds with Pa values ≥ 0.3 were selected. Toxicity screening of the compounds was performed through the web server ProTox II (https://tox-new.charite.de/protox_II/). Parameters used included hepatotoxicity, carcinogenicity, immunogenicity, mutagenicity, and cytotoxicity [13]. The Pa value from bioactivity parameters and the probability active score of cytotoxicity prediction of the selected compounds were then converted into a heatmap.

Molecular Docking

Compounds from the CRE that were selected based on bioactivity and toxicity potential were then used in molecular docking predictions with five target proteins, which are Ikkβ (ID: 4KIK), iNOS (ID: 3E7G), ERK2 (ID: 5BUJ), JNK1 (ID: 3ELJ), and p38 (ID: 6SFO). The three-dimensional (3D) structures of the target proteins were downloaded from the PDB RCSB database (https://www.rcsb.org/). The preparation of target proteins involved the removal of water molecules and non-target ligands using Biovia Discovery Studio 2019. The 3D structures of the compounds were retrieved from the PubChem database (https://pubchem.ncbi.nlm.nih.gov/) and processed with the same software. Molecular docking simulations were conducted using AutoDock Vina integrated within PyRx 0.8. The docking results were visualized using Biovia Discovery Studio 2019[12].

Molecular Dynamics

The protein-ligand complexes obtained from molecular docking were further used for molecular dynamics simulations. Molecular dynamics simulations were performed using YASARA software with the

AMBER14 force field. The parameters used were adjusted to physiological cell conditions, which is 37ºC, pH 7.4, 1 atm pressure, 0.9% salt content, time of 20 ns for the simulation. Analysis parameters used included RMSD, RMSF, and binding energy [12].

Results and Discussion

C. aeruginosa Roxb. Rhizome Ethanol Extract Suppresses NO Production in LPS-Stimulated RAW 264.7 Cells

The measurement of nitrite levels using the Griess method indicated a significant decrease in NO production with increasing concentrations of CRE (Figure 1A). At concentrations of 15, 30, and 60 µL, the nitrite levels decreased to 9.15 µM, 6.11 µM, and 1.84 µM, respectively, corresponding to reductions of approximately 31.4%, 54.2%, and 86.2% relative to the LPS (+) control (13.33 µM). The ethanol extract demonstrated effective inhibition of NO production in a dose-dependent manner, with an IC_{50} value of 29.03 ± 4.37 µg/mL. These findings suggest that CRE significantly suppresses NO production in LPS-stimulated RAW 264.7 macrophages in a concentration-dependent manner. This highlights CRE's potential as a potent anti-inflammatory agent, aligning with its traditional use in managing inflammatory conditions. Notably, NO, a key inflammatory mediator, is synthesized by inducible nitric oxide synthase (iNOS). iNOS plays a major role in propagating inflammatory responses, particularly when produced in excess. Excessive NO production can perpetuate tissue damage and contribute to the pathology of chronic inflammatory diseases.[14] Given that LPS is known to activate canonical inflammatory pathways, including NF-κB and MAPK, our findings suggest that CRE may modulate these pathways, effectively reducing iNOS expression and subsequent NO production[1, 4].

Cell viability test using the WST-1 assay further confirmed that the dose range of CRE did not exhibit cytotoxic effects on RAW 264.7 cell lines, as shown by cell viability percentages consistently above 90% (Figure 1B). The viability assays further confirm CRE's biocompatibility, as RAW 264.7 cells maintained over 90% viability across tested doses, indicating low cytotoxicity and supporting its suitability for therapeutic application. This finding aligns with previous study, [15] indicating that the ethanoic extract of *C. aeruginosa* rhizome has potential as an anti-inflammatory agent, successfully inhibiting NO production at a dose of 25 µg/mL with an inhibition rate exceeding 80%. Furthermore, this result is also consistent with other previous study,[16] who observed that ethanol extract concentrations up to 50 µg/mL not only maintained high cell viability but also reduced pro-inflammatory cytokine production (IL-6, TNF-α) and inhibited macrophage phagocytosis. These cumulative anti-inflammatory effects underscore CRE's potential to modulate multiple inflammatory mediators while preserving cell health, making it a promising candidate for safe anti-inflammatory therapy. Given the promising *in vitro* results, we conducted in silico analyses to explore CRE's bioactive compounds and their specific molecular mechanisms.

Bioactive Compounds Contained in CRE

Given the promising *in vitro* results, we conducted *in silico* analyses to explore CRE's bioactive compounds and their specific molecular mechanisms. Data mining from the literature identified 20 compounds present in the CRE, most of which belong to the sesquiterpene class (Table 1). The CRE, known for its aromatic properties, contains a high proportion of essential oils and volatile compounds, with 64.5% of its essential oils comprising terpenoids. The volatile compound profile primarily includes sesquiterpenes, monoterpenes, esters, and steroids, which are likely to contribute to its anti-inflammatory properties.[9]

Bioactivity and Toxicity Screening of Compounds

The bioactivity screening identified compounds with Pa values predominantly exceeding 0.3, resulting in the selection of 18 candidates that met this threshold (Figure 2A). While compounds with Pa values greater than 0.7 are considered to have a high likelihood of bioactivity, those with Pa values between 0.3 and 0.7 are also classified as active, reflecting a moderate potential for bioactivity. These findings suggest that, despite not demonstrating the highest probability of bioactivity, these compounds may still contribute meaningfully to the observed biological effects and merit further exploration to better understand their therapeutic potential.[17]

The selected bioactive compounds then underwent further screening based on predicted toxicity. According to toxicity predictions, the compound 4, 8-dimethyl-7-octyloxy-2H chromen-2-one was identified with a probability of immunotoxicity and thus was excluded from further analysis (Figure 2B). The final screening yielded a total of 17 compounds (Figure 2C), namely aerugidiol, aeruginolactone, 13-hydroxygermacrone, isoprocurcumenol, procurcumenol, curcolonol, zedoarofuran, curcumenone, germacrone, turmeronol A, turmeronol B, germacrone-13-al, furanogermenone, pyrocurzerenone, dehydrochromolaenin, linderazulene, and curzerenone. These compounds were subsequently used for molecular docking analysis to further investigate their mode of action.

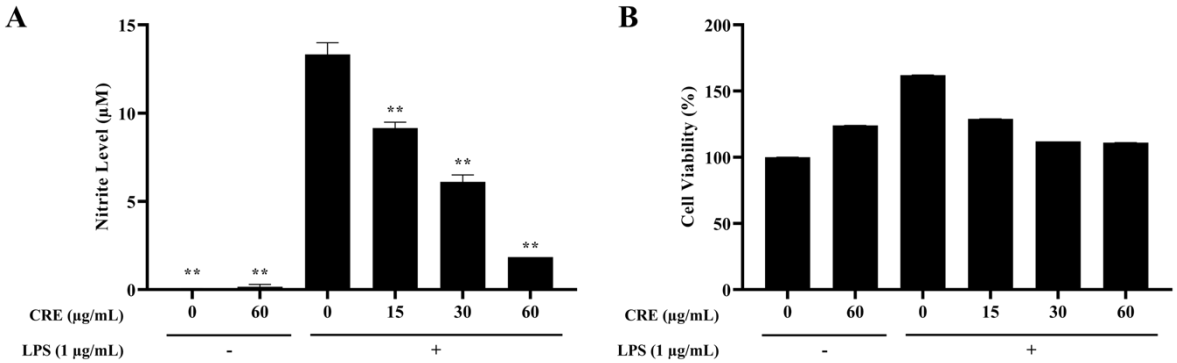

Figure 1: The effects of *C. aeruginosa* Roxb. rhizome ethanol extract (CRE) in LPS-induced RAW 264.7 cells. A) Cells were treated with 1 µg/mL LPS and 15, 30, and 60 µg/mL CRE for 24 hours. NO levels were measured using the Griess assay. The NO levels are expressed as mean ± standard deviation (SD) from triplicate samples. *P < 0.05 and **P < 0.01 compared to the LPS (+) control group. (B) Cell viability was assessed using the WST-1 assay in RAW 264.7 cells treated with different concentrations of CRE for 24 hours. The viability is shown as a percentage relative to the unstimulated control (LPS (-) group). Data are presented as mean ± SD from triplicate samples.

ISSN 2616-0684 (Print)
ISSN 2616-0692 (Electronic)

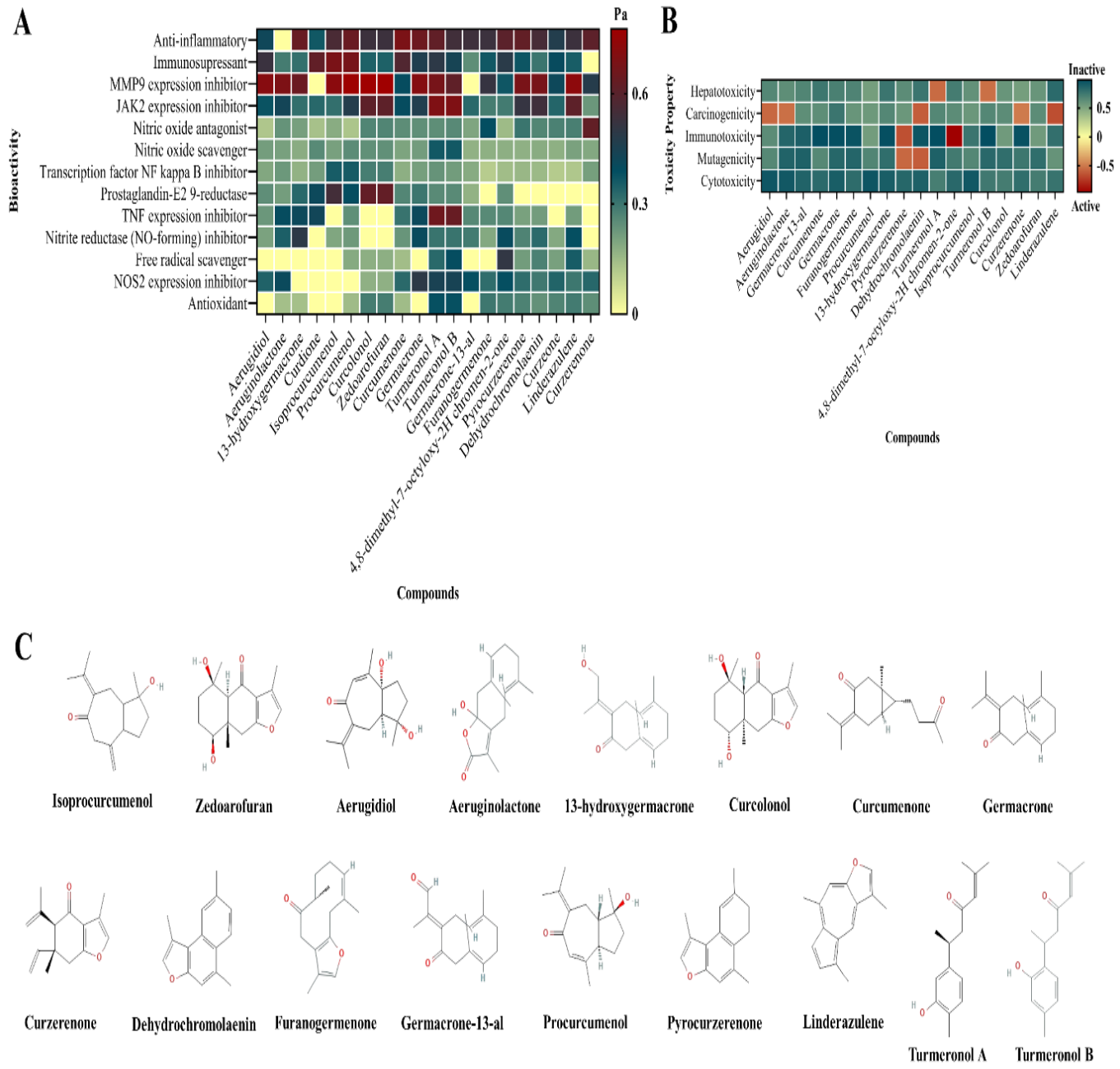

Figure 2: The results of bioactive compound screening of ethanol extract from *C. aeruginosa* rhizome. A) Bioactivity screening, B) toxicity prediction, and C) the 17 compounds that passed both bioactivity and toxicity screening parameters.

Molecular Docking

Molecular docking analysis was conducted to predict the interactions between ligands and target proteins. Ligand-protein complexes with the lowest binding affinities were selected for visualization and further exploration through molecular dynamics simulations. The target proteins chosen for this simulation were Ikkβ (PDB ID: 4KIK), ERK2 (PDB ID: 5BUJ), JNK1 (ID: 3ELJ), p38 (ID: 6SFO), and iNOS (ID: 3E7G). These proteins play pivotal roles in activating pro-inflammatory pathways, ultimately leading to elevated NO levels. For instance, IKKβ activates NF-κB by phosphorylating its inhibitor, IκB, triggering proteasomal degradation and allowing NF-κB to initiate transcription of inflammatory genes.[18] Similarly, MAPK isoforms such as ERK2, JNK1, and p38-α activate AP-1 transcription factors by phosphorylating c-Jun and c-Fos, which bind to promoter regions of pro-inflammatory genes and further enhance NO production.[19, 20] Inhibition of these pathways could therefore significantly reduce NO synthesis, aligning with the observed effects of CRE *in vitro*.

Molecular docking results indicated three potential compounds with the lowest binding affinity values, namely dehydrochromolaenin, pyrocurzerenone, and turmeronol B as competitive inhibitors of key inflammatory proteins. Dehydrochromolaenin binds with Ikkβ (Figure 3A), ERK2 (MAPK1) (Figure 3B), and iNOS (Figure 3E). Furthermore, pyrocurzerenone binds with JNK1 (Figure 3C), and turmeronol B binds with p38 (MAPK14) (Figure 3D). Notably, the iNOS-dehydrochromolaenin complex demonstrated particularly strong binding, as evidenced by its low binding affinity. Binding affinity reflects the free energy of ligand-protein interactions, with lower (more negative) values indicating stronger, more stable binding and higher affinity. Conversely, higher binding affinity values (closer to zero or positive) suggest weaker interactions, which may result in faster ligand dissociation from the protein's active site.[21] These results highlight the

significant potential of dehydrochromolaenin as a stable and effective inhibitor of iNOS activity.

Dehydrochromolaenin interacts with the active site of the Ikk*β* protein via van der Waals forces and four hydrophobic bonds (Figure 4A). It also engages with the ERK2 (MAPK1) protein, forming van der Waals interactions along with four hydrophobic bonds (Figure 4B). Pyrocurzerenone interacts with the active site of JNK1 through van der Waals forces and three hydrophobic bonds (Figure 4C). Similarly, Turmeronol B binds to the active site of p38 (MAPK14) via van der Waals interactions and three hydrophobic bonds (Figure 4D). Furthermore, Dehydrochromolaenin associates with the active site of iNOS, establishing van der Waals forces and three hydrophobic bonds (Figure 4E). These protein-ligand complexes also share interactions with several common residues. Therefore, to evaluate the stability and dynamics of these interactions, molecular dynamics simulations were performed.

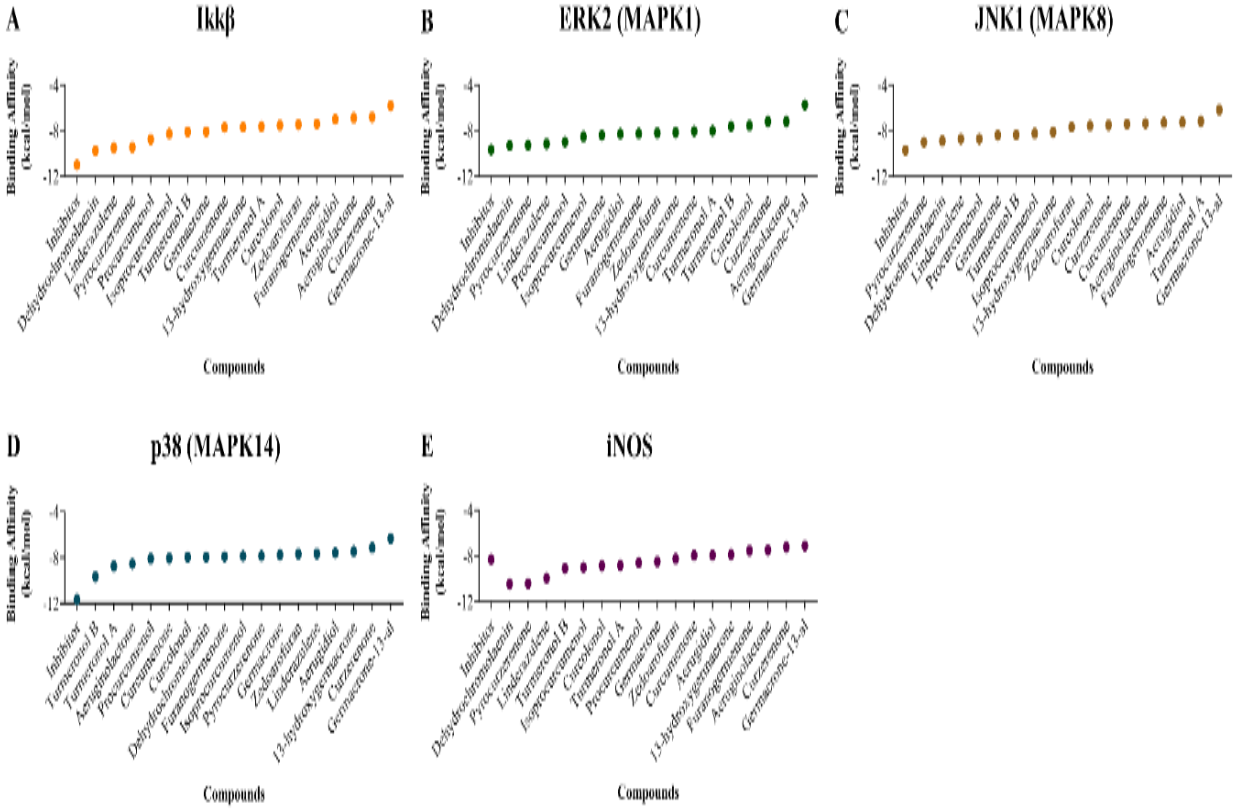

Figure 3: Molecular docking results. Binding affinity score A) IkkB-ligands, B) ERK2-ligands, C) JNK1-ligands, D) p38-ligands, and E) iNOS-ligands.

Molecular dynamics simulations were conducted to analyze the stability of interactions between target proteins and potential compounds from CRE. Simulation parameters included number of hydrogen bond, complex RMSD, ligand conformational RMSD, binding energy, and RMSF. The results showed that the number of hydrogen bonds in protein-inhibitor complexes was greater than in protein-ligand complexes (Figure 5A), suggesting stronger interactions in protein-inhibitor complexes.

Complex RMSD values below 3 Å indicated sufficient interaction stability, [12] as shown in Figure 5B. The Ikk*β*-dehydrochromolaenin complex showed somewhat fluctuating interactions, while the ERK2-dehydrochromolaenin, JNK1-pyrocurzerenone, p38-turmeronol B, and iNOS-dehydrochromolaenin complexes exhibited relatively stable interactions. Although the p38-turmeronol B complex fluctuated from 17 ns (nanoseconds) until 18 ns, it stabilized by the end of the simulation.

The ligand conformational RMSD, which reflects ligand stability in comparison to inhibitors, [22] is shown in Figure 5C. Ligand RMSD values indicated stable interactions across all complexes, similar to those in protein-inhibitor interactions. The Ikk*β*-dehydrochromolaenin, JNK1-pyrocurzerenone, and iNOS-dehydrochromolaenin complexes exhibited lower RMSD values than their inhibitors, while the ERK2-dehydrochromolaenin complex showed comparable stability to its inhibitor. The p38-turmeronol B complex displayed greater stability than its inhibitor. The low RMSD values for ligand conformation suggest that the structure of dehydrochromolaenin remains stable without significant conformational changes throughout the simulation.[23] Overall, all ligand conformational RMSD values were stable.

Positive binding energy values from molecular dynamics indicate increasing stability in protein-ligand complexes.[12] The binding energy fluctuations across all protein-compound complexes remained relatively stable (Figure 5D). Although the p38-turmeronol B complex had a lower binding energy than its inhibitor, its interaction remained stable with minimal fluctuation. The ERK2-dehydrochromolaenin, JNK1-pyrocurzerenone, and iNOS-dehydrochromolaenin complexes demonstrated greater interaction stability than their inhibitors, while the Ikk*β*-dehydrochromolaenin complex exhibited comparable interaction stability.

The RMSF values of the protein-compound complexes displayed fluctuations similar to their respective inhibitors (Figure 6). Notably, the ERK2-dehydrochromolaenin and p38-turmeronol B complexes exhibited minimal fluctuations compared to the Ikk*β*-dehydrochromolaenin, JNK1-pyrocurzerenone, and iNOS-dehydrochromolaenin complexes. Lower RMSF fluctuation of the iNOS-dehydrochromolaenin complex compared to the inhibitor further support dehydrochromolaenin as a potent candidate iNOS inhibitor.[12, 24] Overall, the fluctuations in the protein-compound complexes remained lower than those observed in the protein-inhibitor complexes.

ISSN 2616-0684 (Print)
ISSN 2616-0692 (Electronic)

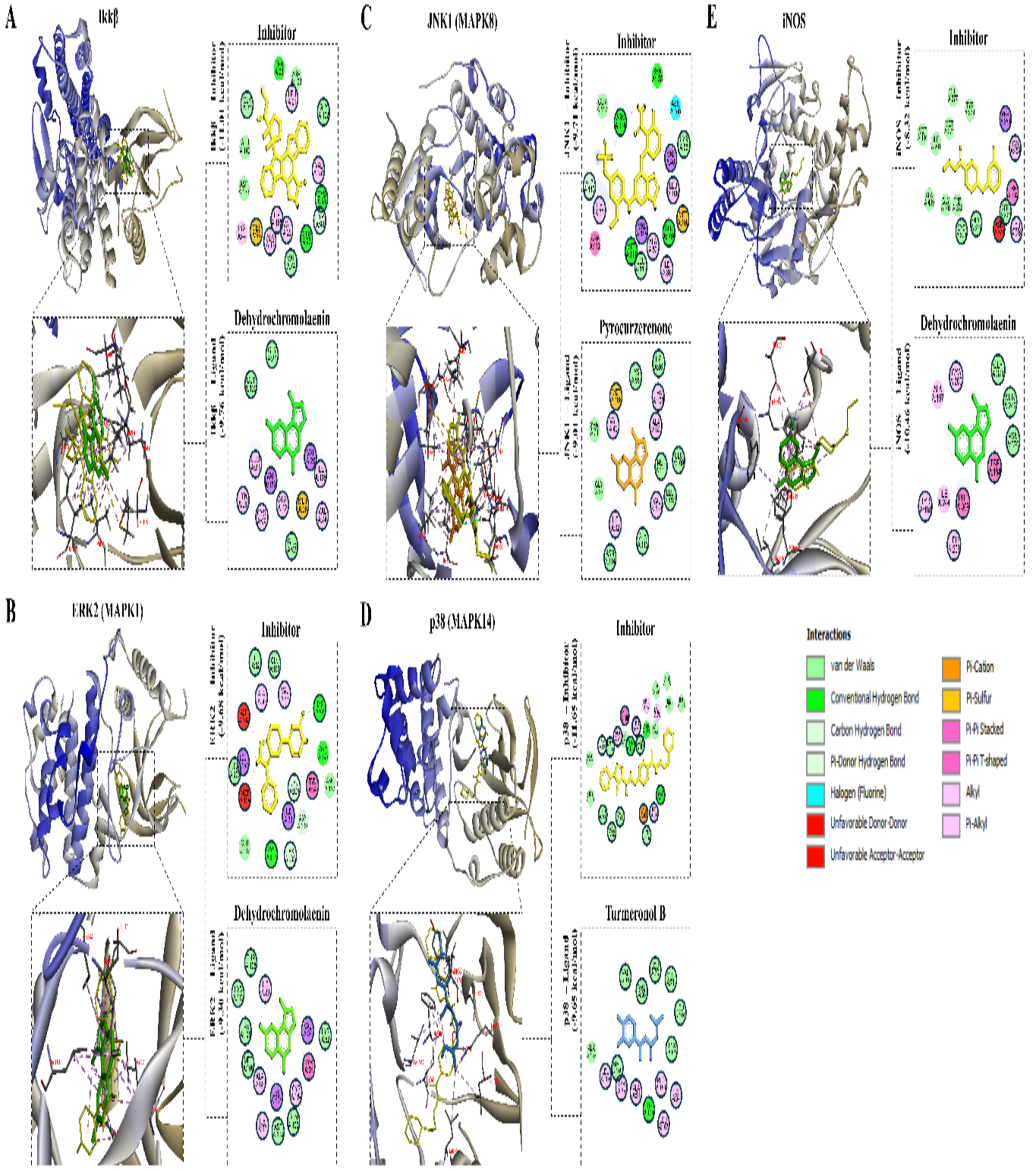

Figure 4: Visualization of interaction between protein and bioactive compound of CRE. A) IkkB-dehydrochromolaenin, B) ERK2-dehydrochromolaenin, C) JNK1-pyrocurzerenone, D) p38-turmeronol B, dan E) iNOS-dehydrochromolaenin. Blue circle indicates the same residue interaction between inhibitor and ligand.

Molecular Dynamic

These insights into CRE's molecular mechanisms add valuable context to its observed *in vitro* effects, highlighting a multifaceted mode of action that likely involves modulating upstream signaling proteins and directly inhibiting NO synthesis. By combining *in vitro* and *in silico* approaches, this study not only corroborates the anti-inflammatory potential of *C. aeruginosa* rhizome extract but also identifies specific bioactive compounds that may be further explored for targeted anti-inflammatory therapies.

ISSN 2616-0684 (Print)
ISSN 2616-0692 (Electronic)

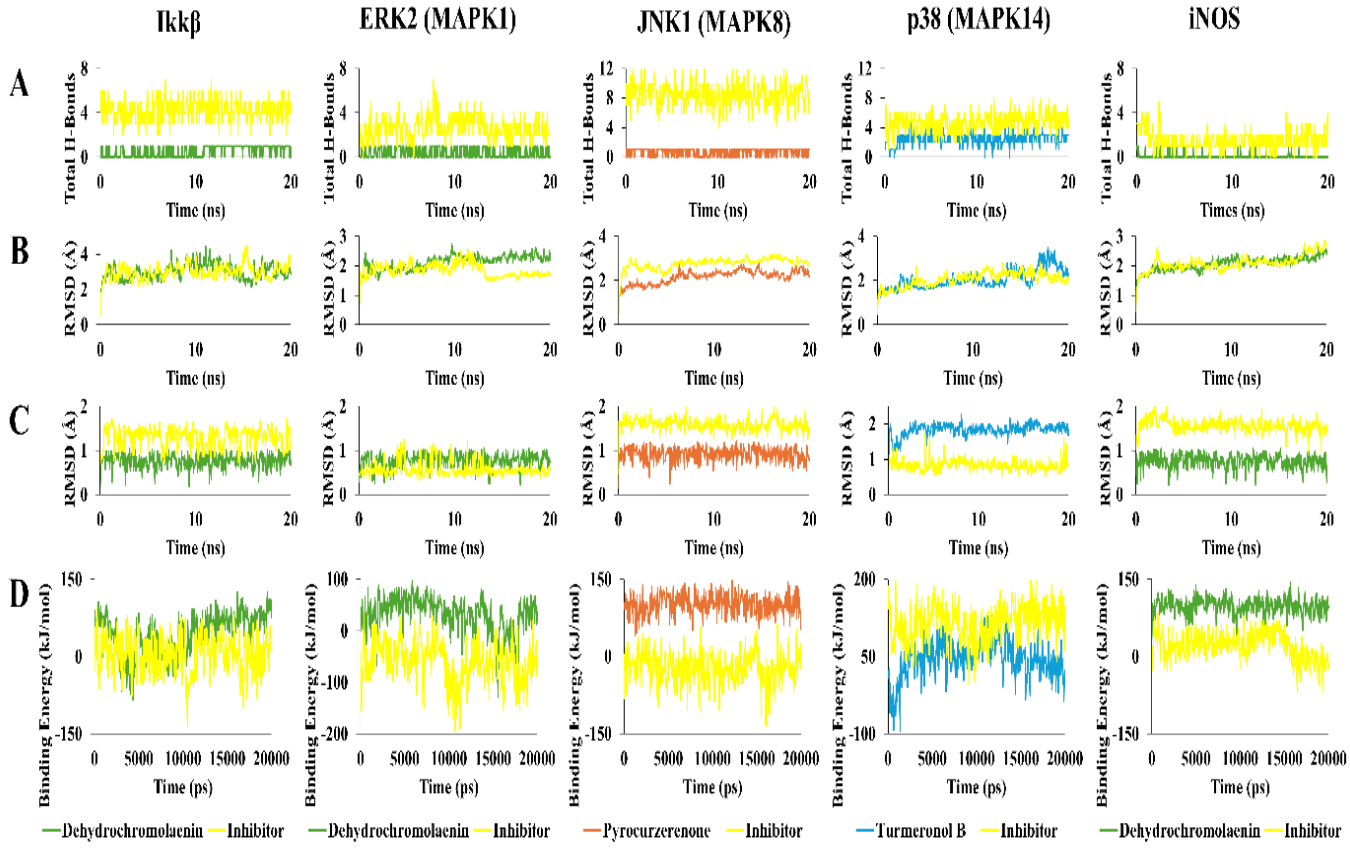

Figure 5: Molecular dynamic simulation of protein-ligand complexes. A) Number of hydrogen bonds, C) Complex RMSD (Root Mean Square Deviation), D) RMSD of ligand conformation, E) binding energy of the complexes.

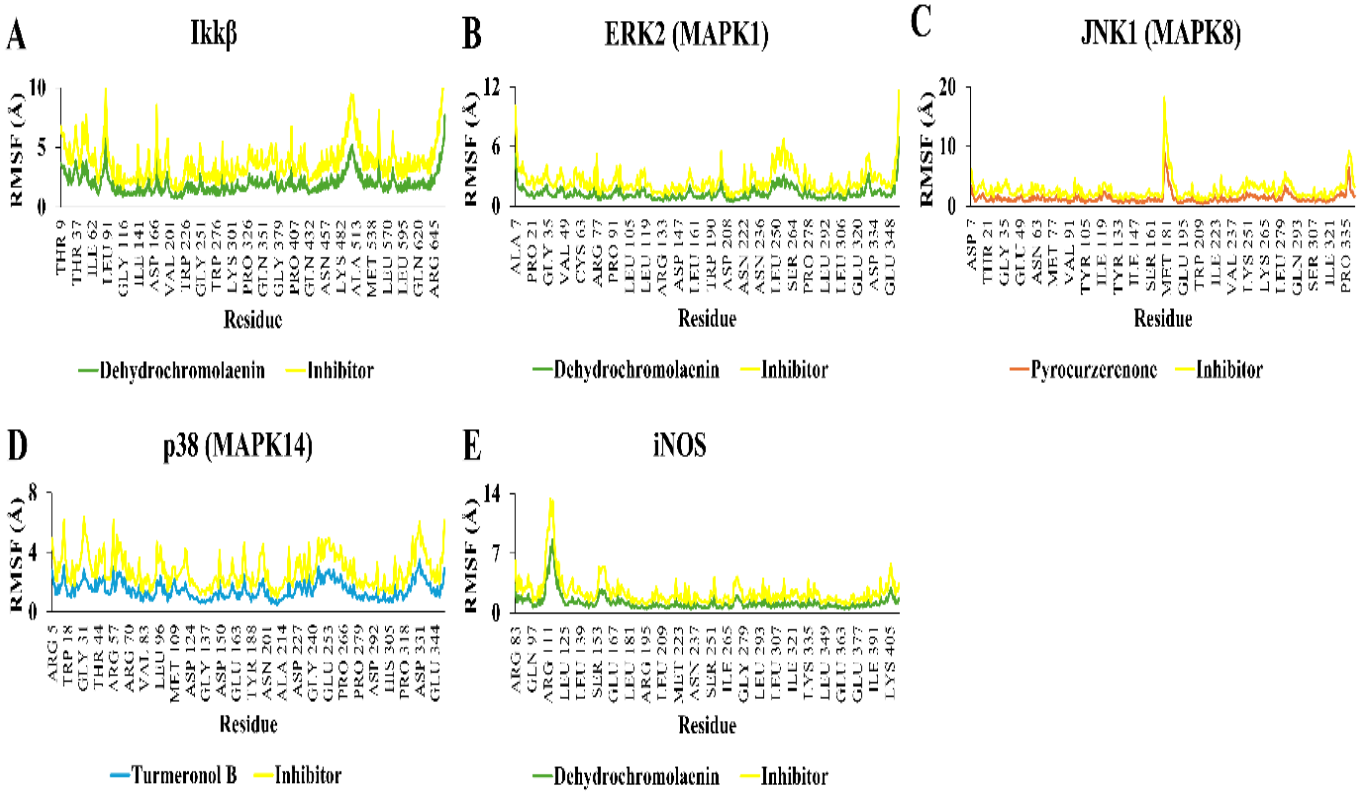

Figure 6: RMSF (Root Mean Square Fluctuation) of molecular dynamic simulation of protein-ligand complexes. RMSF of A) Ikkβ-ligands, B) ERK2-ligands, C) JNK1-ligands, D) p38-ligand, dan E) iNOS-ligands.

Table 1: Bioactive compounds in CRE based on previous study

No.	Compounds	Molecular Formula	PubChem ID	Compound Group	References
1.	Aerugidiol	$C_{15}H_{22}O_3$	11776892	Sesquiterpene	25
2.	Aeruginolactone	$C_{15}H_{20}O_3$	102004678	Sesquiterpene	26
3.	13-hydroxygermacrone	$C_{15}H_{22}O_2$	10399140	Sesquiterpene	27
4.	Cur Dione	$C_{15}H_{24}O_2$	6441391	Sesquiterpene	27
5.	Isoprocurcumenol	$C_{15}H_{22}O_2$	14543197	Sesquiterpene	27
6.	Procurcumenol	$C_{15}H_{22}O_2$	189061	Sesquiterpene	27
7.	Curcolonol	$C_{15}H_{20}O_4$	10683031	Sesquiterpene	27
8.	Zedoarofuran	$C_{15}H_{20}O_4$	11054546	Sesquiterpene	27
9.	Curcumenone	$C_{15}H_{22}O_2$	153845	Sesquiterpene	28
10.	Germacrone	$C_{15}H_{22}O$	6436348	Sesquiterpene	28
11.	Turmeronol A	$C_{15}H_{20}O_2$	11117927	Sesquiterpene	28
12.	Turmeronol B	$C_{15}H_{20}O_2$	10955433	Sesquiterpene	28
13.	Germacrone-13-al	$C_{15}H_{20}O_2$	14633002	Sesquiterpene	28
14.	Furanogermenone	$C_{15}H_{20}O_2$	6439596	Sesquiterpene	28
15.	4,8-dimethyl-7-octyloxy-2H chromen-2-one	$C_{19}H_{26}O_3$	1816934	Phenolic compound	28
16.	Pyrocurzerenone	$C_{15}H_{16}O$	12314812	Sesquiterpene	29
17.	Dehydrochromolaenin	$C_{15}H_{14}O$	12309959	Sesquiterpene	29
18.	Corleone	$C_{15}H_{16}O2$	131751498	Sesquiterpene	29
19	Linderazulene	$C_{15}H_{14}O$	656393	Sesquiterpene	29
20.	Curzerenone	$C_{15}H_{18}O_2$	3081930	Sesquiterpene	29

Conclusion

The CRE showed substantial anti-inflammatory activity by effectively inhibiting NO production in LPS-stimulated RAW 264.7 cells without compromising cell viability. *In silico* analyses further support this finding by identifying stable interactions between key sesquiterpene compounds, such as dehydrochromolaenin, pyrocurzerenone, and turmeronol B and principal proteins in inflammatory signaling pathways, including iNOS, IKKβ, ERK2, JNK1, and p38. Additionally, in silico analysis revealed stable interactions between key bioactive compounds within the extract and primary inflammatory protein targets, particularly iNOS. Thus, CRE showed potential as a natural, effective, and safe alternative for anti-inflammatory therapy. Consequently, CRE presents a valuable, natural alternative with minimized side effects, offering multiple applications in treating inflammation-associated diseases. Future studies should focus on isolating individual compounds and exploring their molecular mechanisms to better understand their role in inflammation suppression. Additionally, further *in vitro* analyses of pro-inflammatory cytokine production could provide insights into CRE's mechanisms and anti-inflammatory effectiveness. To validate its effects under physiological conditions, *in vivo* studies should assess its pharmacokinetics, safety profile, and efficacy in animal models.

Conflict of Interest

The authors declare no conflict of interest.

Authors' Declaration

The authors hereby declare that the work presented in this article is original and that any liability for claims relating to the content of this article will be borne by them.

Acknowledgement

The authors thank to the Animal Physiology Laboratory, Department of Biology, Universitas Brawijaya for supporting this research. The authors also thank the High Performance Computing (HPC) AI-Center UB which has provided HPC facilities for this research. This research also funded by DRTPM (Direktorat Jenderal Pendidikan Tinggi Kementerian Pendidikan dan Kebudayaan Republik Indonesia) through the scheme of Penelitian Fundamental Reguler (PFR) (Grant No. 045/E5/PG/02/00/PL/2024).

References

1. Chen L, Deng H, Cui H, Fang J, Zuo Z, Deng J, Li Y, Wang X, Zhao L. Inflammatory responses and inflammation-associated diseases in organs. Oncotarget. 2018; 9(6):7204-7218. doi:10.18632/oncotarget.23208
2. Jogpal V, Sanduja M, Dutt R, Garg V, Tinku. Advancement of nanomedicines in chronic inflammatory disorders. Inflammopharmacology. 2022; 30(2):355-368. doi:10.1007/s10787-022-00927-x
3. Park YJ, Cheon SY, Lee DS, Cominguez DC, Zhang Z, Lee S, An HJ. Anti-Inflammatory and Antioxidant Effects of *Carpesium cernuum* L. Methanolic Extract in LPS-Stimulated RAW 264.7 Macrophages. Mediators Inflamm. 2020; 2020. doi:10.1155/2020/3164239
4. Tucureanu MM, Rebleanu D, Constantinescu CA, Deleanu M, Voicu G, Butoi E, Calin M, Manduteanu I. Lipopolysaccharide-induced inflammation in monocytes/macrophages is blocked by liposomal delivery of Gi-protein inhibitor. Int J Nanomedicine. 2017; 13:63-76. doi:10.2147/IJN.S150918

5. García-Aranda MI, Gonzalez-Padilla JE, Gómez-Castro CZ, Gómez-Gómez YM, Rosales-Hernández MC, García-Báez EV, Franco-Hernández MO, Castrejón-Flores JL, Padilla-Martínez II. Anti-inflammatory effect and inhibition of nitric oxide production by targeting COXs and iNOS enzymes with the 1, 2-diphenylbenzimidazole pharmacophore. Bioorg Med Chem. 2020; 28(9):115427. doi:10.1016/j.bmc.2020.115427
6. Teslim OA. Side Effects of Non-Steroidal Anti-Inflammatory Drugs: The Experience of Patients with Musculoskeletal Disorders. Am J Health Res. 2014; 2(4):106. doi:10.11648/j.ajhr.20140204.11
7. Thomas Td, Jose S. Comparative phytochemical and anti-bacterial studies of two indigenous medicinal plants *Curcuma caesia* Roxb. and *Curcuma aeruginosa* Roxb. Int J Green Pharm. 2014; 8(1):65. doi:10.4103/0973-8258.126828
8. Siahaan S, Aryastami NK. Policy Study on the Development of Medicinal Plants in Indonesia. Health Research and Development Media. 2018; 28(3):157-166. doi:10.22435/mpk.v28i3.119
9. Sari AP, Supratman U. Phytochemistry and Biological Activities of *Curcuma aeruginosa* (Roxb.). Indones J Chem. 2022; 22(1):576. doi:10.22146/ijc.70101
10. Djati MS, Christina YI, Rifa'i M. The combination of *Elephantopus scaber* and *Sauropus androgynus* promotes erythroid lineages and modulates follicle-stimulating hormone and luteinizing hormone levels in pregnant mice infected with *Escherichia coli*. Vet World. 2021:1398-1404. doi:10.14202/vetworld.2021.1398-1404
11. Dwijayanti DR, Widyananda MH, Hermanto FE, Soewondo A, Afiyanti M, Widodo N. Revealing the anti-inflammatory activity of *Euphorbia hirta* extract: transcriptomic and nitric oxide production analysis in LPS-Induced RAW 264.7 cells. Food Agric Immunol. 2024; 35(1). doi:10.1080/09540105.2024.2351360
12. Widyananda MH, Wicaksono ST, Rahmawati K, Puspitarini S, Ulfa SM, Jatmiko YD, Masruri M, Widodo N. A Potential Anticancer Mechanism of Finger Root (*Boesenbergia rotunda*) Extracts against a Breast Cancer Cell Line. Scientifica (Cairo). 2022; 2022:1-17. doi:10.1155/2022/9130252
13. Widyananda MH, Muflikhah L, Ulfa SM, Widodo N. Unveiling the antibreast cancer mechanism of *Euphorbia hirta* ethanol extract: computational and experimental study. J Biol Act Prod Nat. 2024; 14(3):359-382. doi:10.1080/22311866.2024.2361684
14. Lind M, Hayes A, Caprnda M, Petrovic D, Rodrigo L, Kruzliak P, Zulli A. Inducible nitric oxide synthase: Good or bad? Biomed Pharmacother. 2017; 93:370-375. doi:10.1016/j.biopha.2017.06.036
15. Andrina S, Churiyah C, Nuralih N. Anti-Inflammatory Effect of Ethanolic Extract of *Curcuma aeruginosa* Roxb Rhizome, *Morinda Citrifolia* Fruit and *Apium graveolens* Leaf on Lipopplysaccharide-induce RAW 264.7 Cell Lines. Indones J Cancer Chemoprevent. 2017; 6(3):84. doi:10.14499/indonesianjcanchemoprev6iss3pp84-88
16. Dewi IP, Dachriyanus, Aldi Y, Ismail NH, Hefni D, Susanti M, Syafri S, Wahyuni FS. *Curcuma aeruginosa* Roxb. Extract Inhibits the Production of Proinflammatory Cytokines on RAW 264.7 Macrophages. Int J Appl Pharm. 2024:41-44. doi:10.22159/ijap.2024.v16s1.08
17. Iqbal M, Kurniawan RV, Nurfani HDW, Roestamadji RI, Luthfi M, Setyowati D, Setijanto RD, Surboyo MDC. Molecular docking analysis of major active compounds of pomegranate peel extract (*Punica granatum* L.) in inhibiting cyclooxygenase enzyme. World J Adv Res Rev 2023; 20(3):1824-1842. doi:10.30574/wjarr.2023.20.3.2653
18. Gamble C, McIntosh K, Scott R, Ho KH, Plevin R, Paul A. Inhibitory kappa B kinases as targets for pharmacological regulation. Br J Pharmacol. 2012; 165(4):802-819. doi:10.1111/j.1476-5381.2011.01608.x
19. Hegazy MEF, Hamed AR, Mohamed TA, Debbab A, Nakamura S, Matsuda H, Paré PW. Anti-inflammatory sesquiterpenes from the medicinal herb *Tanacetum sinaicum*. RSC Adv. 2015; 5(56):44895-44901. doi:10.1039/C5RA07511D
20. Wang Y, Jia Q, Zhang Y, Wei J, Liu P. Amygdalin Attenuates Atherosclerosis and Plays an Anti-Inflammatory Role in ApoE Knock-Out Mice and Bone Marrow-Derived Macrophages. Front Pharmacol. 2020; 11. doi:10.3389/fphar.2020.590929
21. Josaphat F, Fadlan A. Molecular Docking of Acetylacetone-Based Oxindole Against Indoleamine 2, 3-Dioxygenase: Study of Energy Minimization. Walisongo J Chem. 2023; 6(2):149-157. doi:10.21580/wjc.v6i2.17638
22. Marseti SW, Hermanto FE, Widyananda MH, Rosyadah N, Kamila FS, Annisa Y, Dwijayanti DR, Ulfa SM, Widodo N. Pharmacological potential of *Clinacanthus nutans*: integrating network pharmacology with experimental studies against lung cancer. J Biol Active Prod Nat. 2024; 14(3):343-358. doi:10.1080/22311866.2024.2367997
23. Odhar HA. Molecular docking and dynamics simulation of FDA approved drugs with the main protease from 2019 novel coronavirus. Bioinformation. 2020; 16(3):236-244. doi:10.6026/97320630016236
24. Abdullah A, Putri NTM, Rosyadah N, Ramadhani P, Putri SAK, Widyananda MH, Kurniawan N, Fatchiyah F. The Study of flavonoid in *Apium graveolens* L. as a Kirsten Rat Sarcoma Protein Inhibitor in Colorectal Cancer based on *in silico* Study. Biotropika. 2023; 11(2):115-124. doi:10.21776/ub.biotropika.2023.011.02.07
25. Masuda T, Jitoe A, Nakatani N. Structure of Aerugidiol, a New Bridge-head Oxygenated Guaiane Sesquiterpene. Chem Lett. 1991; 20(9):1625-1628. doi:10.1246/cl.1991.1625
26. Sirat HM, Jamil S, Hussain J. Essential Oil of *Curcuma aeruginosa* Roxb. from Malaysia. J Essent Oil Res. 1998; 10(4):453-458. doi:10.1080/10412905.1998.9700942
27. Otsuka H, Minh Giang P, Tong Son P, Matsunami K. New Sesquiterpenoids from *Curcuma aeruginosa* Roxb. Heterocycles. 2007; 74(1):977. doi:10.3987/COM-07-S(W)42
28. Suharsanti R, Astuti P, Yuniarti N, Wahyuono S. Review of Isolation Methods, Chemical Composition and Biological Activities of *Curcuma aeruginosa* Roxb Rizhome. Trop J Nat Prod Res. 2022; 6(10):1538-1546. doi:10.26538/tjnpr/v6i10.1
29. Boutsada P, Giang VH, Linh TM, Mai NC, Cham PT, Hanh TTH, Phonenavong K, Sengchanh S, Cuong NX, Lien LQ, Ban NK.. Sesquiterpenoids from the rhizomes of *Curcuma aeruginosa*. Vietnam J Chem. 2018; 56(6):721-725. doi:10.1002/vjch.201800077